Instrument for measuring the misalignments of ocular surfaces

Juan Tabernero, Antonio Benito, Vincent Nourrit and Pablo Artal

Laboratorio de Óptica, Departamento de Física, Universidad de Murcia, Campus de Espinardo (Edificio CiOyN), 30071 Murcia Spain

juant@um.es, abenito@um.es, vnourrit@um.es, pablo@um.es

Abstract: A compact and robust instrument for measuring the alignment of ocular surfaces has been designed and used in living eyes. It is based on recording Purkinje images (reflections of light at the ocular surfaces) at nine different angular fixations. A complete analysis on the causes of misalignments of Purkinje images and its relations with those physical variables to be measured (global eye tilt, lens decentration and lens tilt) is presented. A research prototype based on these ideas was built and tested in normal and pseudophakic eyes (after cataract surgery). The new analysis techniques, together with the semicircular extended source and multiple fixation tests that we used, are significant improvements towards a robust approach to measuring the misalignments of the ocular surfaces in vivo. This instrument will be of use in both basic studies of the eye's optics and clinical ophthalmology.

OCIS codes: (330.5370) Physiological optics; (170.4460) Ophthalmic optics.

References and Links

1. J. Liang, B. Grimm, S. Goelz, and J.F. Bille. "Objective measurement of wave-aberration of the human eye with the use of a Hartmann Shack wave-front sensor," J. Opt. Soc. Am. A. **11**, 1949-1957 (1994).
2. P.M. Prieto F. Vargas-Martín, S. Goelz, and P. Artal, "Analysis of the performance of the Hartmann-Shack sensor in the human eye," J. Opt. Soc. Am. A. **17**, 1388-1398 (2000).
3. A. Guirao, and P. Artal, "Corneal wave aberration from videokeratography: accuracy and limitations of the procedure," J. Opt. Soc. Am. A. **17**, 955-965 (2000).
4. P. Artal, A. Guirao, E. Berrio, and D.R. Williams, "Compensation of corneal aberrations by internal optics in the human eye," J. Vis. **1**, 1-8 (2001).
5. P. Artal, E. Berrio, A. Guirao, and P. Piers, "Contribution of the cornea and internal surfaces to the change of ocular aberrations with age," J. Opt. Soc. Am. A. **19**, 137-143 (2002).
6. Y. Le Grand, and S. G. El Hage, *Physiological Optics* (Springer Verlag, Berlin 1980).
7. P. Phillips, J. Pérez-Emmanueilli, H.D. Rosskothen, and C.J. Koester "Measurement of intraocular lens decentration and tilt in vivo," J. Cataract. Refract. Surg. **14**, 129-35 (1988).
8. J.D. Auran, C.J. Koester, and A. Donn, "In vivo measurement of posterior chamber intraocular lens decentration and tilt," Arch. Ophthalmol. **108**, 75-79 (1990).
9. J.C. Barry, K. Branman, and M.C.M. Dunne, "Catoptric properties of eyes with misaligned surfaces studied by exact ray tracing," Invest. Ophthalmol. Vis. Sci. **38**, 1476-1484 (1997).
10. J.C. Barry, M.C.M. Dunne, and T. Kirschkamp, "Phakometric measurement of ocular surface radius of curvature and alignment: evaluation of method with physical model eyes," Ophthalmic Physiol. Opt. **21,** 450-460 (2001).
11. T. Kirschkamp, M.C.M. Dunne, and J.C. Barry, "Phakometric measurement of ocular surface radii of curvature axial separation and alignment in relaxed and accommodated human eyes," Ophthalmic Physiol. Opt. **24**, 65-73 (2004).
12. P. Rosales, and S. Marcos, "Phakometry and lens tilt and decentration using a custom-developed Purkinje imaging apparatus: validation and measurements," J. Opt. Soc. Am. A **23**, 509-520 (2006).
13. D.L. Guyton, H. Uozato, and H.J. Wisnicki, "Rapid determination of intraocular lens tilt and decentration through the undilated pupil," Ophthalmology **97,** 1259-1264 (1990).
14. R.Navarro, M.Ferro, P.Artal, and I.Miranda, "Modulation transfer-functions of eyes implanted with intraocular lenses," Appl. Opt. **32,** 6359-6367 (1993).
15. J. Tabernero, P. Piers, A. Benito, M. Redondo, and P. Artal, "Predicting the optical performance of eyes implanted with IOLs correcting spherical aberration," Inv.Ophthalmol.Vis.Sci. **47**, 4651-4658 (2006).

#74494 - $15.00 USD Received 29 August 2006; revised 10 October 2006; accepted 20 October 2006

16. J.E. Kelly, T. Mihashi, and H.C. Howland, "Compensation of corneal horizontal/vertical astigmatism, lateral coma, and spherical aberration by internal optics of the eye," J. Vis. **4,** 262-271 (2005).
17. P. Artal, A. Benito, and J. Tabernero, "The human eye is an example of robust optical design," J. Vis. **6,** 1-7 (2006).

1. Introduction

In recent years, the advent of improved techniques for measuring aberrations of the eye permitted a more detailed and complete understanding on the optics of the human eye [1,2]. By combining data on the ocular and corneal aberrations [3], the relative contribution of the crystalline lens to the eye's aberration was determined [4]. It was shown that the lens in most young eyes compensates, at least in part, for the aberrations associated to the cornea, although this compensation tends to vanish with age [5]. However, how the actual aberrations of the lens are produced within the eye is not yet completely understood. To answer this question, we need to have a better knowledge of the geometrical parameters of the crystalline lens. From the early days of Physiological Optics, the main source of information from the lens was that available by collecting and analyzing the reflections from the ocular surfaces, i.e.; the Purkinje images [6]. Moreover, in different aspects of clinical Ophthalmology, it is important to measure the ocular surfaces misalignments, for example after implantation of intraocular lenses (IOLs) in cataract surgery.

If the eye is a well-centered optical system and we align an illumination source with its optical axis, we would expect to see four well-centered images formed by reflection of the light source at the ocular interfaces (air-cornea, cornea-aqueous, aqueous-lens, lens-vitreous). First and second Purkinje images (air-cornea (PI) and cornea-aqueous (PII)) have similar size and are usually overlapped, due to the small corneal thickness. Aqueous-lens reflection (PIII) has the largest size (approximately twice of PI) and lens-vitreous reflection (PIV) is usually slightly smaller in size than PI, but it is inverted with respect to the others. Images PI and PIV are formed in planes near the pupil plane, while PIII has its focus beyond the lens in the vitreous. Figure 1 shows a simulated reflection pattern of a semicircular source (an array of LEDs) in a perfectly centered eye model. All three reflections are symmetrically centered.

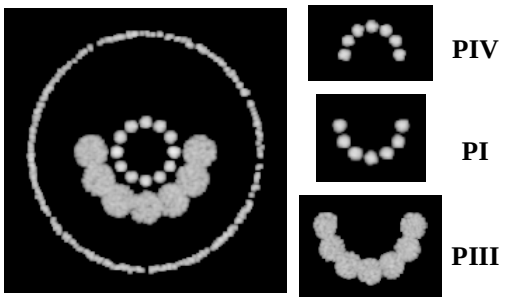

Fig. 1. Pupil edge and Purkinje images of a semicircular source (array of LEDs) in a perfectly aligned model eye.

However, when a real human eye fixates to a point, Purkinje images are typically seen misaligned. There are three possible causes for this misalignment to occur: a global eye rotation, lens decentration and lens tilt (Fig. 2). These three causes are physiologically plausible and will act in combination. Phillips et al. [7] proposed a lineal model that relates the positions of Purkinje images to eye rotation, lens tilt and lens decentration. This model has also been used by several authors [8-12]. A more clinically oriented method to assess misalignments in eyes implanted with an intraocular lens was also described [13]. It is based on locating the superposition of images PIII and PIV that marks the optical axis. We describe here a simple but precise and robust approach to measuring the position of the crystalline lens, or implanted IOLs. The method is based on recording the Purkinje images of a particular

#74494 - $15.00 USD Received 29 August 2006; revised 10 October 2006; accepted 20 October 2006

target for a series of different controlled fixations of the subject. A description of the apparatus, the processing method and examples of results in different eyes are presented.

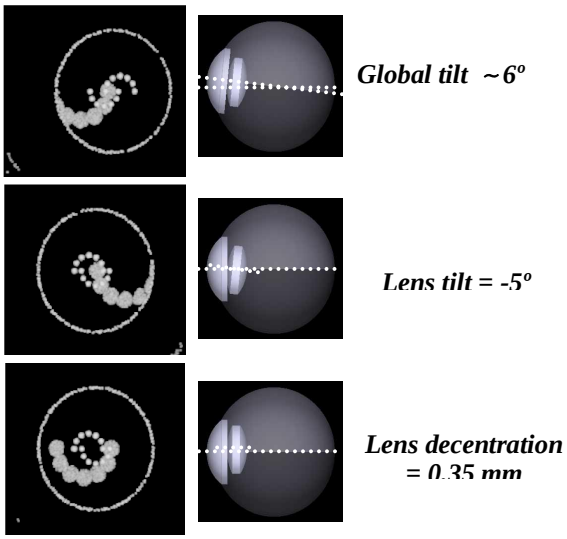

Fig. 2. Global eye tilt, lens tilt and lens decentration cause Purkinje images generated by a semicircular source to be misaligned.

2. Methods

2.1 Theory

It is important to specify first those axes used to define the alignment of the ocular surfaces. To avoid confusion, in the following we will treat only with the two more relevant and measurable axes: the *principal line of sight*, (the line from the center of the entrance pupil that passes through the fixation point) and the *pupillary axis* (the line perpendicular to the cornea that also passes through the center of the entrance pupil) (Fig. 3).

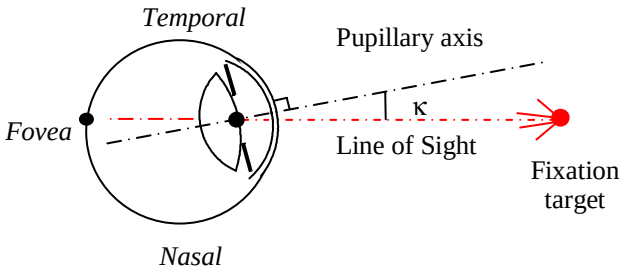

Fig. 3. Schematic representation of angle kappa. It is important to note that due to angle kappa the lens is systematically tilted with respect to the line of sight.

Both axes are non coincident in normal subjects. The angle between these axes is usually denoted as kappa (although it can be also referred as lambda). It has an average value around 5 degrees [6]. The origin of this misalignment can be understood because of the location of the fovea, normally with a temporal tendency with respect to the most approximate optical axes. As it was mentioned above, alignment of PI, PIII and PIV is not possible in a general case with a combination of general eye rotation, lens decentration and lens tilt. If all three reflections are observed aligned when the eye fixates to the source, then the system cornea-

#74494 - $15.00 USD Received 29 August 2006; revised 10 October 2006; accepted 20 October 2006

lens-fovea would be perfectly lined-up. However it is always possible to align PIII and PIV (i.e. lens reflections) by moving a source in front of the eye and therefore change eye's fixation. In the clinic [13] usually a light source is moved in front of the eye to locate the overlapping position of PIII and PIV. The angular distance from that light to the line of sight (fixation point) when overlapping occurs approximates lens tilt (with respect to the line of sight).

Moreover the distance from the geometrical pupil centre to the overlapping point gives an estimation of lens decentration. Similarly, the source can be aligned coaxially with the line of sight and ask the subject to fixate to a series of previously established angular positions. We denote $\beta_{AL\ PIII+PIV}$ the eye rotation required to align PIII and PIV. In the most general case this rotation must compensate for the three different factors that generate the misalignment between PIII and PIV:

i) the eye might be globally rotated when fixating to a point source. This is a systematic effect due to angle kappa (see fig. 3). The rotation required to compensate for this factor is denoted as $\beta_{Global\ Rot.}$

ii) the lens might be tilted with respect to the pupillary axis. A rotation required to compensate for this factor is denoted as $\beta_{Lens\ Tilt}$

iii) a decentration of the lens with respect to the pupil will require a rotation to align PIII and PIV that is denoted as $\beta_{Lens\ Dec.}$

The combination of the three factors yields:

$$\beta_{AL\ PIII+PIV} = \beta_{Global\ Rot.} + \beta_{Lens\ Tilt} + \beta_{Lens\ Dec.} \quad (1)$$

It is important to note that this equation separates the effect of a global eye rotation from lens tilt (that is given with respect to the pupillary axis). If the eye fixates to a point source and we refer lens tilt to the line of sight, then a lens tilt value would already exist, owing to the global eye rotation generated by angle kappa. The equation above could be rewrite as

$$\beta_{AL\ PIII+PIV} = \beta_{Lens\ Tilt(LoS)} + \beta_{Lens\ Dec.} \quad (2)$$

where we have referred lens tilt to the Line of Sight (LoS), and then it already includes the offset generated by the global rotation (angle kappa). In order to provide the most complete description of the ocular alignment, in the following we will use Eq. 1, referring lens tilt to the pupillary axis. We need to make some assumptions to introduce the parameters to be calculated into the equation. In particular we suggest a linear relationship between rotations and their causes. Thus we can rewrite the equation as

$$\beta_{AL\ PIII+PIV} = \beta_{Global\_Rot.} + A_1 Tilt + A_2 Dec \quad (3)$$

There are two unknown coefficients in this equation. A_1 represents the angular rotation that an eye must do to compensate for one degree of lens tilt (in the absence of global rotations and decentration). A_2 represents the angular rotation that an eye must do to compensate for a separation between PIII and PIV caused by 1 mm of lens decentration (in the absence of global rotations and lens tilt). To further study the validity of this linear relationship and to calculate both A_1 and A_2, we used a ray-tracing program (ZEMAX Development Corp, San Diego, CA) to simulate in an eye model the positions of the Purkinje images for different realistic situations. Fig. 4 shows the positions of PIII and PIV for the Le Grand's eye model when the lens is tilted and after the eye rotation that aligns both. For computational simplicity, we used a point source to generate PIII and PIV, instead of the semicircular ring of LEDs of previous figures. Similarly, amounts of decentration (0.5, 1 and 1.5 mm) were introduced and the global rotations required to align PIII and PIV were calculated. The results are shown in fig. 5-A (calculation of A_1) and 5-B (calculation of A_2). Both parameters, A_1 and A_2, depend slightly on corneal angular magnification within the range of physiologically possible corneal powers (36 D to 45 D). However when we change corneal parameters within physiological possible ranges, we found very little variation. Therefore, we assumed that the values calculated from the Le Grand eye model are good enough in practice. We chose a value of 1.1 for A_1 and 2.0 (degrees×mm^{-1}) for A_2. Let

#74494 - $15.00 USD Received 29 August 2006; revised 10 October 2006; accepted 20 October 2006

suppose that we illuminated the eye coaxially with the line of sight and we ask the subject to fixate to different, and well established, angular positions, recording the position of the reflections with a camera placed coaxially with the illumination source. By linear fitting, it can be extrapolated the eye rotation that the eye should perform to overlap PIII and PIV. In other words, we measured $\beta_{AL\ PIII+PIV}$. In addition, from the distance of the overlapping position to the center of the entrance pupil, the decentration of the lens is obtained (the third term of Eq. (1): $\beta_{Lens\ Dec.}$). To separate out the effects of a global rotation (say angle kappa) from lens tilt with respect to the pupillary axis, a way to measure it is necessary. An option is to align the corneal reflex with the center of the entrance pupil. This angular overlapping position is relatively easy to estimate, once the subject has fixated to the series of angular targets, in a similar way as we calculated the overlapping position for PIII and PIV. This provides $\beta_{Global\ Rot.}$. Finally, it only remains to estimate $\beta_{Lens\ Tilt}$ from Eq. (1) to determine the lens tilt with respect to the pupillary axis.

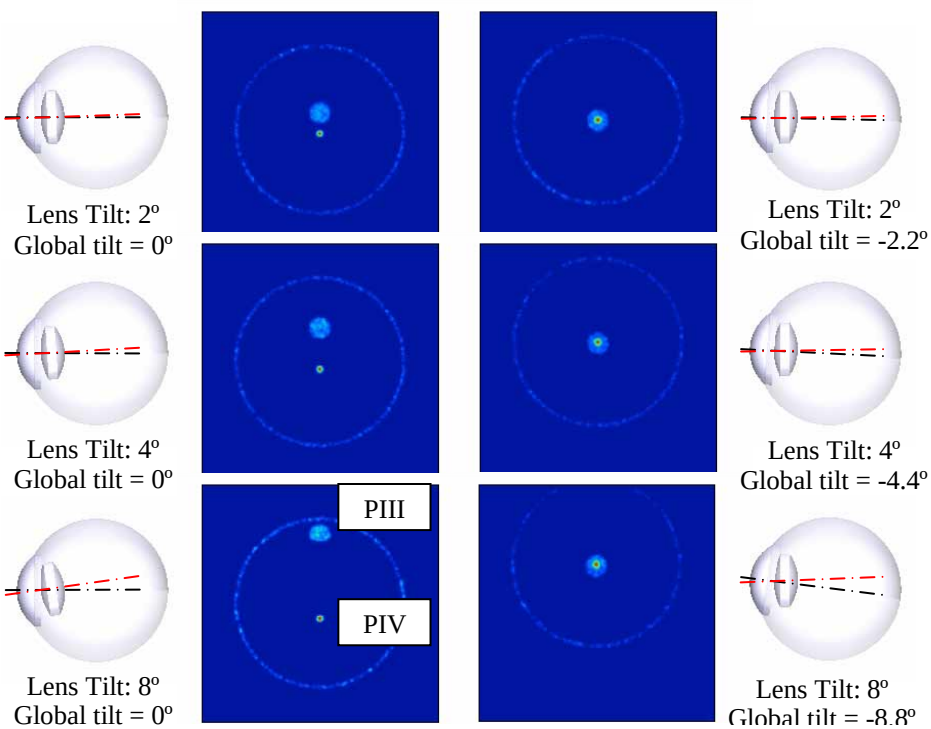

Fig. 4. On the left column, Purkinje images III and IV generated by a point source are represented for different lens tilts (2, 4 and 8 degrees). On the right column, the same Purkinje images are represented after a global eye tilt that aligns both.

#74494 - $15.00 USD Received 29 August 2006; revised 10 October 2006; accepted 20 October 2006

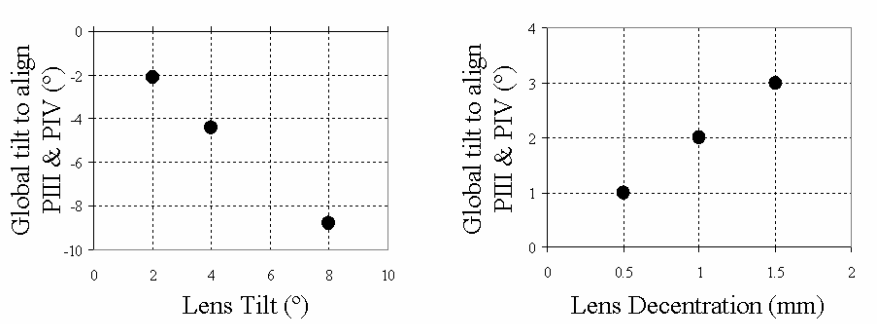

Fig. 5. The global eye tilt required to align PIII and PIV as a function of lens tilt (on the left) and lens decentration (on the right).

2.2 Experimental set-up

We built a prototype to practically implement the ideas described in the previous section. Figure 6 shows two different views of the experimental system. The instrument was mounted over a movable base containing a chin and forehead rest used to hold the head of the subject steady during the measurements. A semicircular array of infrared LEDs was used to illuminate the eye (A) co-aligned with a telecentric camera objective (B) and a CCD camera (C) that records the Purkinje images produced by this source. The use of a semicircular source has some advantages with respect to a point source to generate Purkinje images. First it has a non symmetric geometry which easily allows identification of Purkinje images (PIII and PIV are inverted with respect to each other). Also the use of this extended source allows the location of Purkinje images even when they are partially vignetted by the pupil. Nine fixation red LEDs were designed to symmetrically cover a central visual field (extreme LEDs are separated by 10.4 degrees, see image).

The central fixation LED was aligned with the CCD-Lens axis. The measurement procedure begins with centering the eye's pupil. While the subject fixates at the central LED its pupil is approximately centered within the CCD recording area. This is a way to align the line of sight with the instrument axis. The CCD camera was conjugated with the iris plane. One image of the anterior part of the eye was recorded for each fixation positions. Custom image processing software was used to determine the location of the Purkinje images with respect to the center of the entrance pupil (fitted to an ellipse).

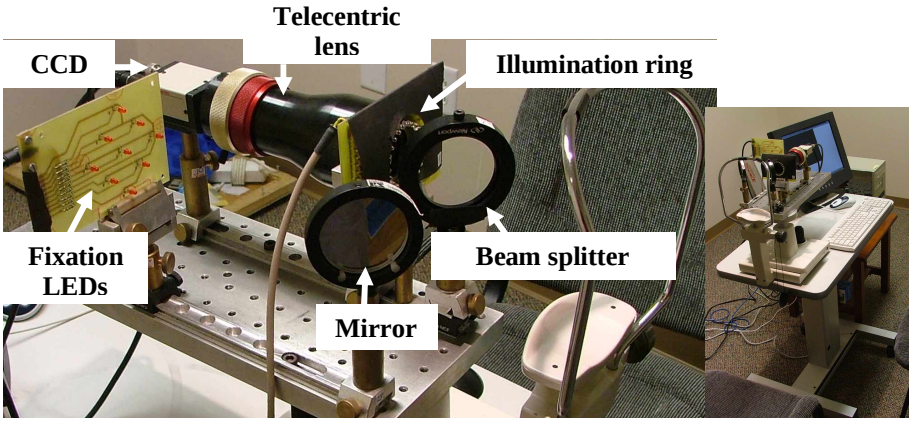

Fig. 6. Photographs of the experimental prototype.

#74494 - $15.00 USD Received 29 August 2006; revised 10 October 2006; accepted 20 October 2006

3. Results

3.1 Computer simulations

A computational modeling of our experimental system was performed using Zemax software. This allowed us to investigate in advance many different "virtual" experiments and to search for the best configuration parameters. Figure 7 shows an example of the analysis performed. An eye model with given values of angle kappa (6, 2)º, lens tilt (-4, 2)º and lens decentration (0.4, -0.3) mm was rotated simulating five eye fixations, in horizontal directions: ((0, 0)º, (4, 0)º, (-4, 0)º) and vertical directions: ((0, 4)º, (0, -4)º), similarly to the actual situation in the instrument.

For each of these fixations, the position of each Purkinje image with respect to the pupil was calculated and plotted against rotations (Fig. 8). The PI line represents positions of the corneal reflex as a function of eye rotation. When it crosses through the X-axis, pupil centre and corneal reflex are overlapped, which provides with the value of angle kappa. The PIII and PIV line are the positions of both images with respect to the center of the entrance pupil as a function of rotations. The overlapping point of lens reflections is given from the interception point of these two lines. The Y-coordinate of this point is an estimation of the lens decentration with respect to pupil center and the X-coordinate represents the overlapping eye rotation $\beta_{AL\ PIII+PIV}$. Results obtained from these images were all very similar to the nominal values: Tilt = (-3.8, 1.9) (º); Dec = (0.39, -0.33) (mm); Angle kappa = (5.9, 2.1) (º).

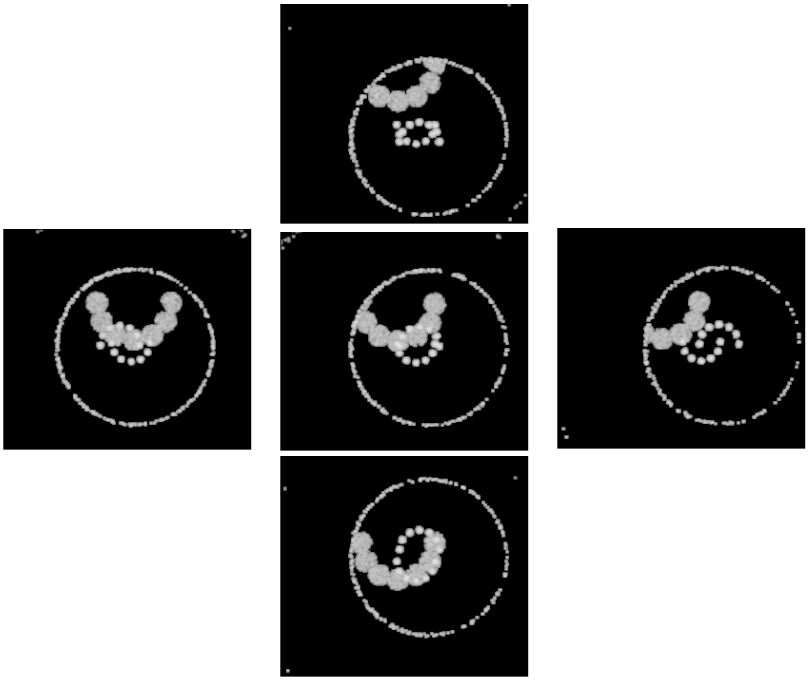

Fig. 7. Simulations of Purkinje images in an eye model with nominal values of tilt and decentration for different eye rotations simulating fixations at five different angular positions.

#74494 - $15.00 USD Received 29 August 2006; revised 10 October 2006; accepted 20 October 2006

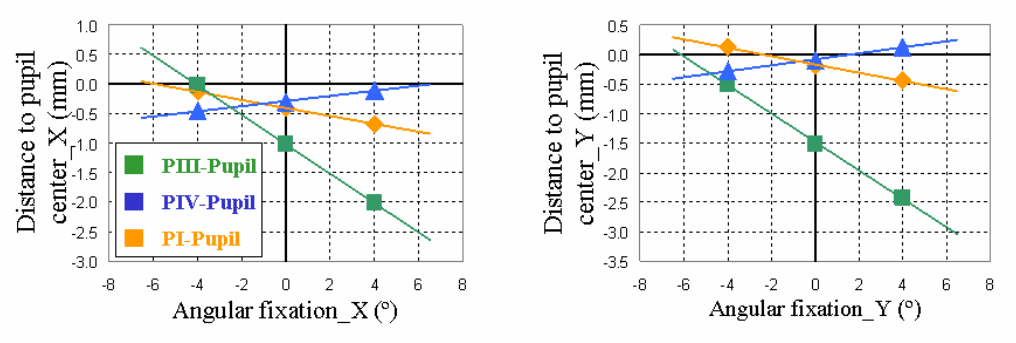

Fig. 8. The position of each Purkinje image with respect to the pupil is plotted versus angular rotations in both horizontal and vertical directions.

3.2 Pseudophakic eyes

The instrument was first applied in eyes with implanted intraocular lenses after cataract surgery. This had the advantage that the reflections were brighter than in the real eye, and that the geometrical data of the lenses were precisely known. The IOL implanted was the Ceeon 911A model (AMO, Santa Ana, USA), a foldable lens with a 6 mm optical zone and a refractive index of 1.458. Purkinje images were nicely visualized in these eyes. As an example two movies for two patients are presented in Figs. 9(a) and 9(b). Linear fittings of positions versus rotations for horizontals and vertical coordinates are depicted in Fig. 10 (patient psdhk_1_os). These plots were used to calculate the tilt and intraocular lens decentration and also ocular angle kappa using the procedure described above.

We obtained the next values in the two eyes:

psphk_1_os: Angle kappa = (3.0, 1.4) (º); IOL Tilt = (-1.9, 1.2) (º); IOL decentration = (-0.21, 0.15) mm

psphk_2_od: Angle Kappa = (7.6, 2.7) (º); IOL Tilt = (0.7, 2.0) (º); IOL decentration = (0.29, -0.05) mm

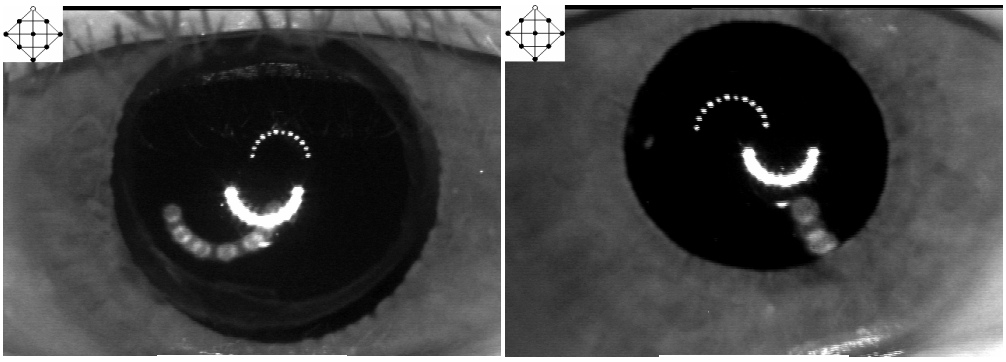

(a) (b)

Fig. 9. Movies of the measurement sessions from the two pseudophakic eyes included in this work. The positions of the Purkinje images change with the fixation target (upper left corner in each movie).

#74494 - $15.00 USD Received 29 August 2006; revised 10 October 2006; accepted 20 October 2006

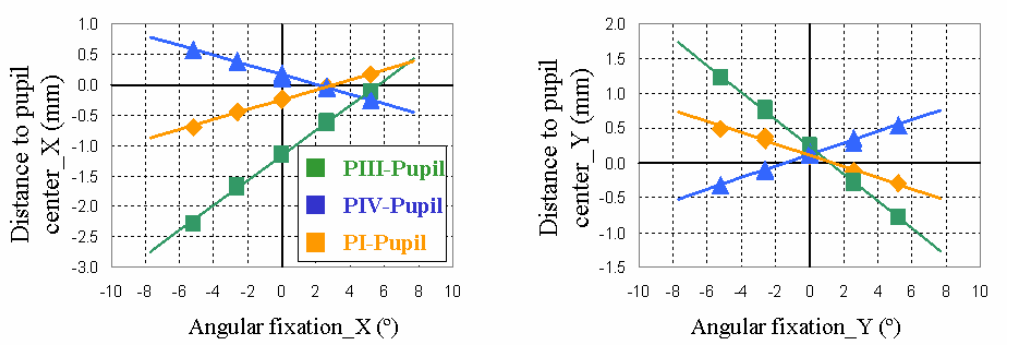

Fig. 10. The positions of each Purkinje image with respect to the entrance pupil center versus angular fixation for the first pseudophakic eye in both horizontal and vertical direction.

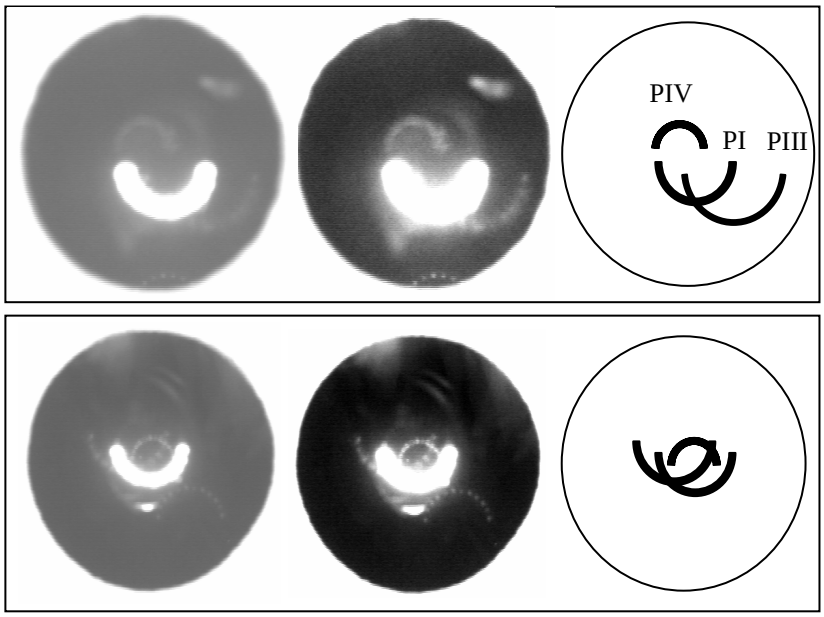

Fig. 11. Visualizing PI, PIII and PIV for the two normal eyes included in this study. The third column is a schematic draw of the position of each Purkinje image.

3.3 Normal eyes

We present here as another example, results from two normal eyes (ages 26 and 50 years old). Both were measured using their natural pupil size. There were some reasons to expect a worse signal-to-noise ratio in the natural lens reflections in comparison with the IOL reflections of the previous section. First, the refractive index of the crystalline lens (around 1.42) is lower than the IOL refraction index (1.458). In addition in the natural lens, the third Purkinje image is rather diffuse as compared with a specular reflection in the IOLs. These factors were especially relevant when recording PIII. The reflectance of PIII and PIV have similar values, but the magnification is approximately twice for PIII. This means that approximately the same (small) amount of energy is distributed over a larger area, reducing the signal. Despite these

#74494 - $15.00 USD Received 29 August 2006; revised 10 October 2006; accepted 20 October 2006

difficulties, it was possible to clearly detect PIII in most normal eyes (see Figs. 11(a) and 11(b) as an example for two normal eyes). The actual analysis consisted on superimpose an ellipse over each Purkinje image. The location was done separated for each Purkinje image, so PIII and PI were not located with the same digital enhancement. For example, the central images in Fig. 11 were adequate to locate PIII and PIV, but not for PI which appeared too blurred for this condition. The corneal reflection (PI) was therefore better located using the images on the left hand side of Fig. 11. With appropriate digital enhancement of the images it was feasible to accurately locate the position of PIII. Some other reflections that appear in the images are due to spurious multiple reflections and were not considered in the analysis. Figure 12 shows the linear fitting of the locations of Purkinje images to the rotations in one of the subjects (nrm_1_od). The measured values for both subjects were:
nrm_1_od: Angle Kappa = (6, -1.8) (º); Lens Tilt = (2.4, -0.9) (º); lens decentration = (-0.08, 0.06) mm
nrm_2_os: Angle kappa = (2.4, 0.3) (º); Lens Tilt = (-2.8, 0.3) (º); lens decentration = (0.02, 0.13) mm

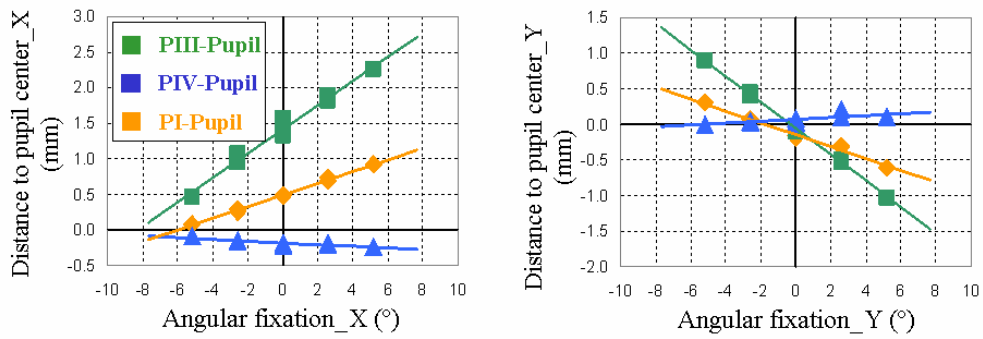

Fig. 12. The positions of each Purkinje image with respect to the entrance pupil center versus angular fixation for the first normal eye included in this study in both horizontal and vertical direction.

3.4 Estimation of the experimental error

The experimental reliability of the method relied on the quality of the linear fittings of eye rotations against Purkinje image positions. Although linearity was well assumed in the ranges of tilt and decentration that are physiologically possible, subjects might erroneously fixate to the angular targets. The detection of the pupil and Purkinje positions also contributes with some amount of uncertainty to the linear fittings. Therefore to determine the experimental error we must analyze the quality of the linear fitting performed. In particular we must estimate the uncertainty of the interception point of two straight lines (which is required to calculate decentration and tilt) and the uncertainty of the interception point of a straight line with the Y = 0 axis (required to get angle kappa).

The coordinates (X_C, Y_C) of the interception point of two linear regressions

$$\begin{aligned} Y &= a_1 X + b_1 \\ Y &= a_2 X + b_2 \end{aligned} \tag{4}$$

will be obtained from the next formulas:

$$\begin{aligned} X_C &= -\left(\frac{b_1 - b_2}{a_1 - a_2}\right) \\ Y_C &= a_1 X_C + b_1 \end{aligned} \tag{5}$$

Each slope and intercept has their own standard error from the regression analysis Δa_1, Δa_2, Δb_1 and Δb_2. To calculate ΔX_C, ΔY_C we must derivate as:

#74494 - $15.00 USD Received 29 August 2006; revised 10 October 2006; accepted 20 October 2006

$$\Delta X_C = \left|\frac{\partial X_C}{\partial a_1}\right|\Delta a_1 + \left|\frac{\partial X_C}{\partial a_2}\right|\Delta a_2 + \left|\frac{\partial X_C}{\partial b_1}\right|\Delta b_1 + \left|\frac{\partial X_C}{\partial b_2}\right|\Delta b_2$$
$$\Delta Y_C = \left|\frac{\partial Y_C}{\partial a_1}\right|\Delta a_1 + \left|\frac{\partial Y_C}{\partial b_1}\right|\Delta b_1 + \left|\frac{\partial Y_C}{\partial X_C}\right|\Delta X_C \tag{6}$$

From here we can finally write

$$\Delta X_C = \frac{1}{|a_1 - a_2|}\left[|X_C|(\Delta a_1 + \Delta a_2) + (\Delta b_1 + \Delta b_2)\right]$$
$$\Delta Y_C = |X_C|\Delta a_1 + \Delta X_C |a_1| + \Delta b_1 \tag{7}$$

It could be interesting to note that the uncertainty in the calculus of the interception point increases when the difference of slopes decreases. In the limit of equal slopes (parallel lines) the uncertainty is infinity. As it was also expected, the uncertainty is proportional to the error of each regression.

ΔX_C represents the angular error in the determination of the PIII and PIV overlapping point while ΔY_C gives the uncertainty in position for that point. Therefore they can be taken as the uncertainty for lens/IOL tilt and decentration.

The estimation of the error in angle kappa comes from the uncertainty in the X-axis intercept of a linear regression. This intercept is given by:

$$X_C = -\frac{b}{a} \tag{8}$$

From here we can easily write the uncertainty of X_C as a function of the uncertainty of the linear regression parameters, b and a:

$$\frac{\Delta X_C}{|X_C|} = \frac{\Delta a}{|a|} + \frac{\Delta b}{|b|} \tag{9}$$

Figure 13 shows the experimental errors calculated by this method in the subjects we measured here. All the decentration uncertainties were well below 0.1 mm and tilt and kappa uncertainties were no larger than 0.8 degrees. Average uncertainties for the components of decentration were 0.03 mm and around 0.3 degrees for the components of tilt and angle kappa.

4. Conclusions

A new instrument for measuring the alignment of the ocular surfaces in vivo has been developed. It is suitable for both clinical and research applications. It is based on the recording of Purkinje images for different fixations and subsequent adequate analysis. The method allows separation of the effects of a global eye tilt (angle kappa) from a lens tilt with respect to the optical axis of the pupil-cornea optical system (i.e. the pupillary axis). The procedure to obtain lens tilt and decentration from Purkinje images originally proposed by Phillips et al. [7] required to specify nine constants that represents the movement of each Purkinje image per unit of parameter that induce it (i.e. eye rotation, lens tilt and lens decentration). In our approach, only two constants are required. One potential advantage of Phillips´ and similar method was the use of one single image containing the set of Purkinje images. However we favored the option of recording multiple images what renders the methods more robust and accurate. Our computer simulations and error analysis suggest that the procedure provides data accurate enough for visual optics research.

#74494 - $15.00 USD Received 29 August 2006; revised 10 October 2006; accepted 20 October 2006

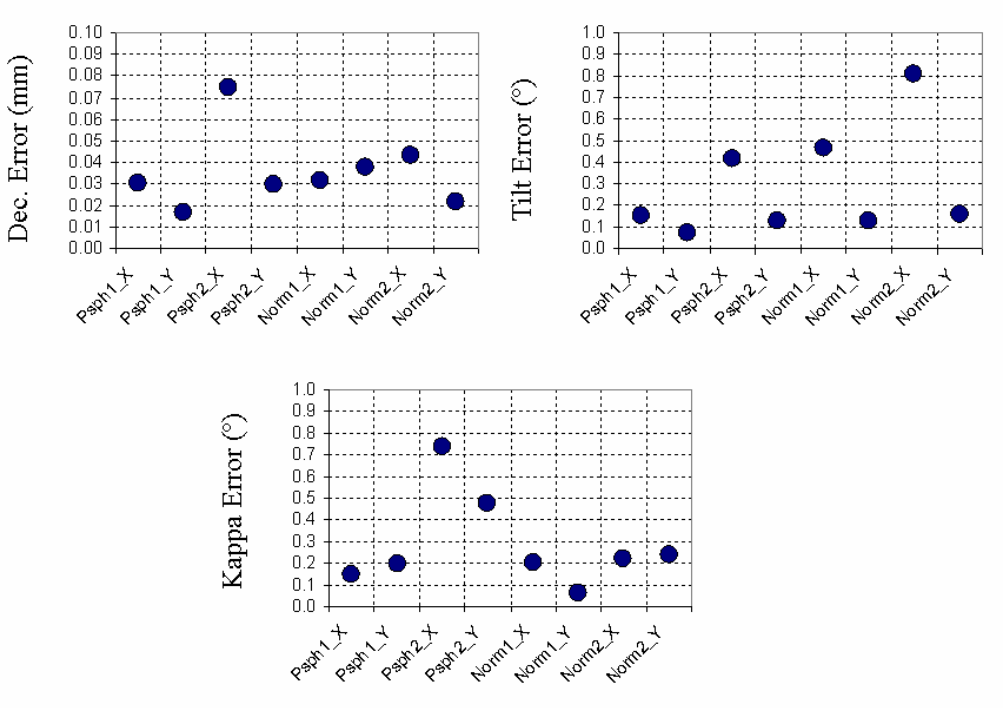

Fig. 13. Uncertainties in the measurement of each component of tilt, decentration and kappa angle for the four eyes included in this study.

The instrument and procedure analysis has been successfully applied to pseudophakic patients. It is interesting to note that IOL misalignments are an extremely relevant application area for this instrument. Retinal image quality [14] can be potentially affected in eyes implanted with misaligned intraocular lenses, in particular those with aspheric profiles [15]. A precise control of the decentration and tilts of IOLs after cataract surgery will be a key issue to further improve future lenses and surgical techniques.

We have also demonstrated the potential use of the instrument in normal eyes. Although the clinical relevance for normal eyes is not straightforward (maybe for checking strabismus or exotropia), the instrument has capabilities to further investigate the relationships between the alignment of the ocular surfaces and retinal image quality. Some recent research already addressed the impact of ocular alignment for the compensation of aberrations within the eye [16,17].

In summary, we have described an instrument for measuring the alignment of the optical components of the eye in vivo, either the cornea plus the crystalline lens, or the cornea plus an intraocular lens. The instrument is robust and provides accurate data with potential in clinical and research applications.

Acknowledgments

This study was supported in part by "Ministerio de Educación y Ciencia", Spain (grant FIS2004-2153) and the "Sharp-Eye" European Union RTN (fellowship to VN).

#74494 - $15.00 USD Received 29 August 2006; revised 10 October 2006; accepted 20 October 2006